Supplementary Information (SI) for RSC Advances.

Electronic Supplementary Information (ESI)

Controlled Colloidal Synthesis and Structure–Property–Stability Relationships of Lead-Free $CsMBr_3$ Nanocrystals

S.N. Ngwenya, K.P. Mubiayi*, N. Moloto*

School of Chemistry, University of the Witwatersrand
Private Bag 3
Wits 2050, South Africa

Corresponding authors: Kalenga P Mubiayi; Nosipho Moloto

Email: Kalenga.Mubiayi@wits.ac.za; Nosipho.Moloto@wits.ac.za

Tel: +27 11 717 6720; +27 11 717 6774

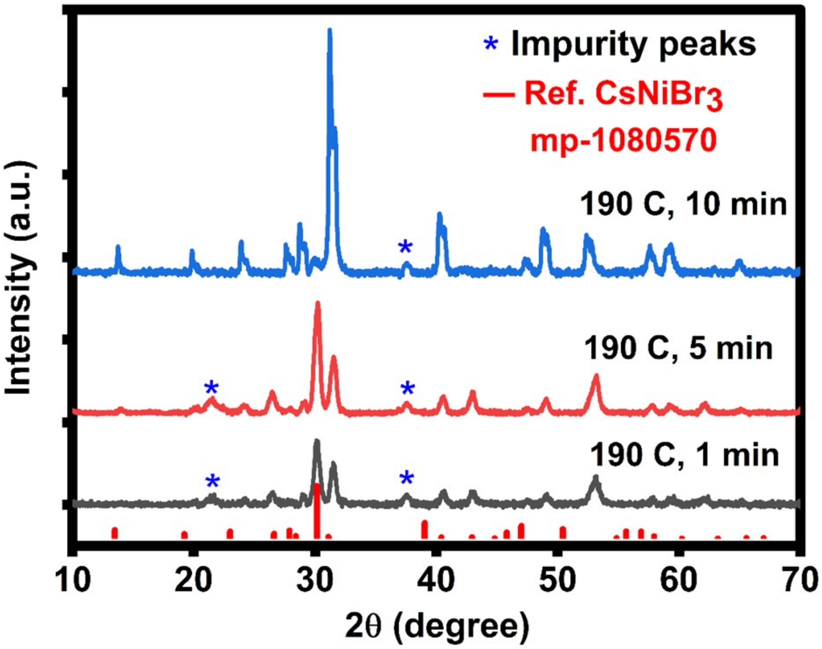

Fig. S1. P-XRD patterns of synthesized $CsNiBr_3$ samples prepared at 190 °C for different reaction times (1, 5, and 10 min). The diffraction peaks are compared with the reference pattern of $CsNiBr_3$ (mp-1080570), indicated by the red vertical bars. Peaks marked with (*) correspond to impurity phases. The results show the evolution of crystallinity and phase purity with increasing reaction time.

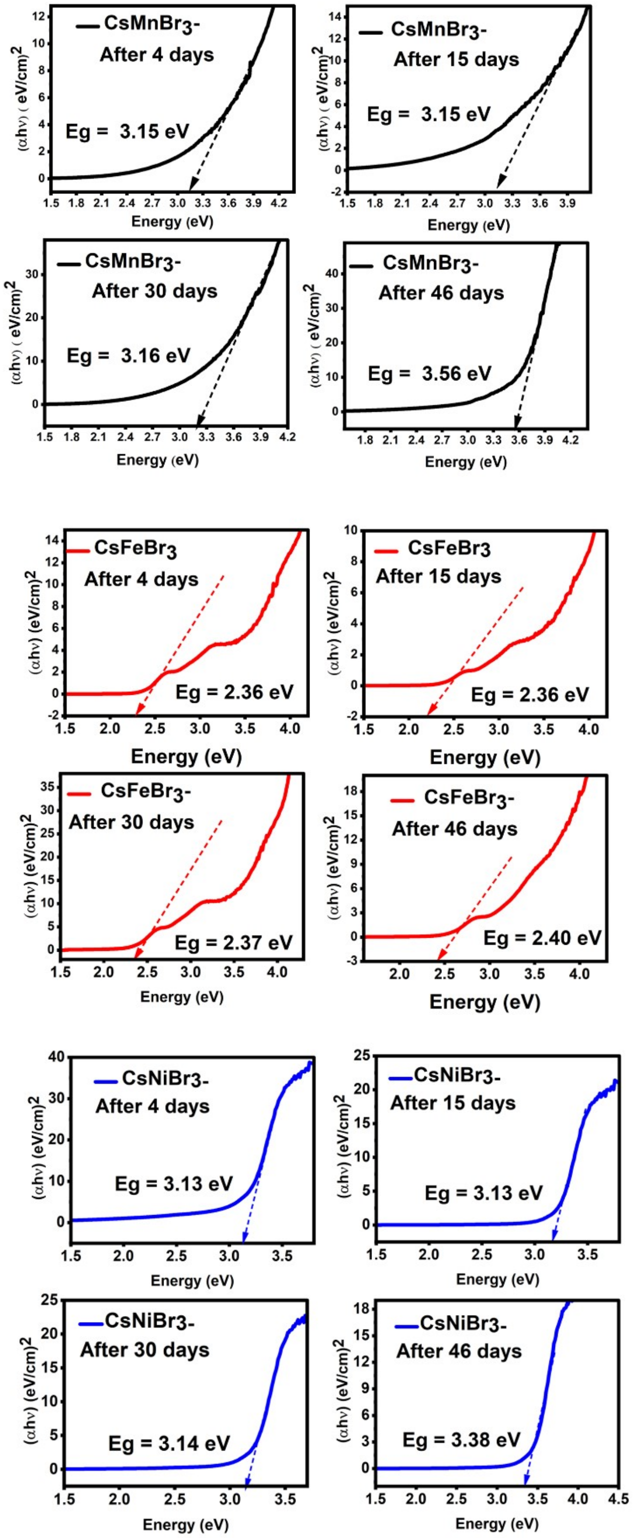

Fig. S2. Tauc plots of $CsMBr_3$ (M = Mn, Fe, Ni) for the determination of the optical band gaps. The plot shows $(\alpha h\nu)^2$ versus photon energy $h\nu$. The band gap Eg is estimated by extrapolating the linear region of the plot to $(\alpha h\nu)^2 = 0$.

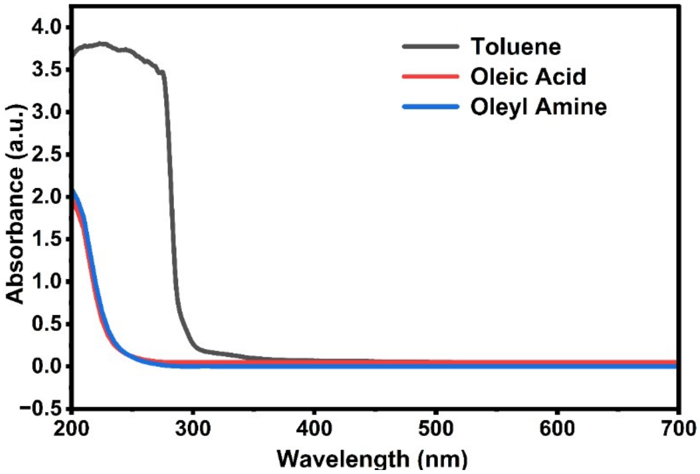

Fig. S3. UV-vis absorption spectra of toluene (used as the solvent for UV-vis measurements), oleic acid (OA), and oleylamine (OLA) used in the synthesis of $CsMBr_3$ nanocrystals. The spectra were measured separately as control references to confirm that the absorption features of the nanocrystals are not contributed by the solvent or ligands.

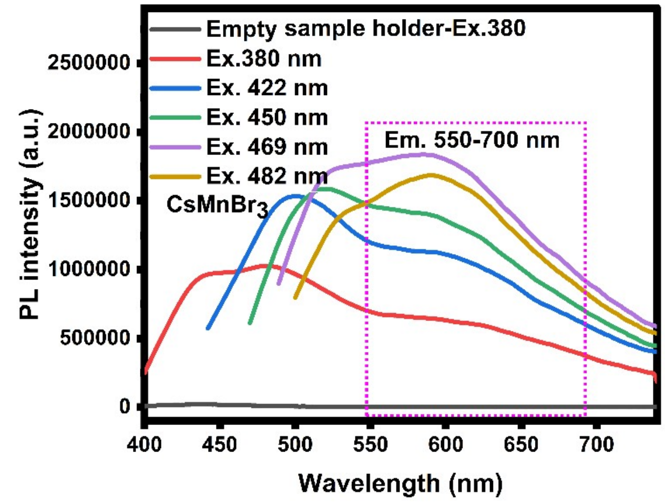

Fig. S4. PL emission spectra of $CsMnBr_3$ nanocrystals recorded under different excitation wavelengths (380, 422, 450, 469, and 482 nm). The grey curve represents the empty sample holder measured at 380 nm for background correction. The spectra exhibit a broad emission band in the 550 - 700 nm region (highlighted), indicating strong visible luminescence with no significant peak shift upon changing the excitation wavelength.

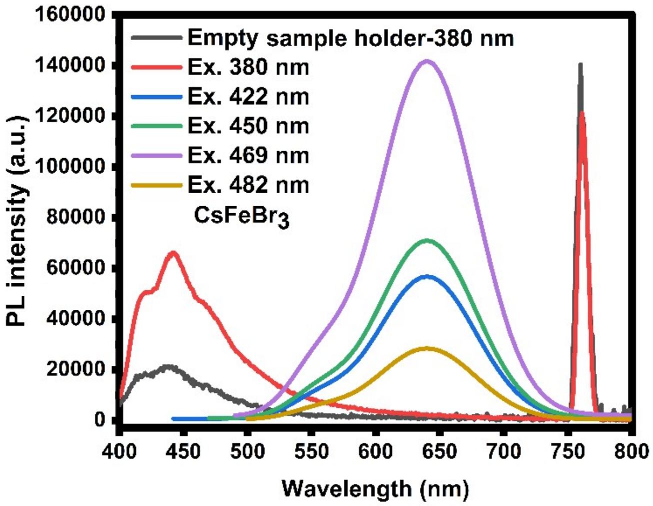

Fig. S5. PL emission spectra of $CsFeBr_3$ nanocrystals recorded under different excitation wavelengths (380, 422, 450, 469, and 482 nm). The grey curve represents the empty sample holder measured at 380 nm for background correction. The spectra dual emission band in the 550 - 750 nm region, indicating strong visible luminescence with no significant peak shift upon changing the excitation wavelength.

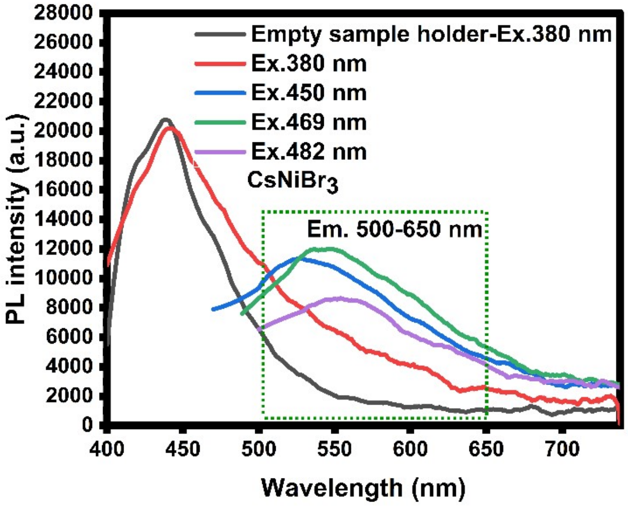

Fig. S6. PL emission spectra of $CsNiBr_3$ nanocrystals recorded under different excitation wavelengths (380, 450, 469, and 482 nm). The grey curve represents the empty sample holder measured at 380 nm for background correction. The spectra dual emission band in the 500 - 650 nm region, indicating a very weak luminescence with small peak shift upon changing the excitation wavelength.

Average lifetime calculation

For TRPL, the average lifetime was calculated as:

$$\tau_{avg} = \frac{A_1\tau_1^2 + A_2\tau_2^2}{A_1\tau_1 + A_2\tau_2}$$

This represents an effective recombination lifetime. Where, τ_1 short-lifetime resulting from excitonic radiative recombination, τ_2 long-lifetime from trapped-assisted non-radioactive recombination. A_0 represents constants, $\mathbf{A_1}$ and $\mathbf{A_2}$ are the weights of multiple exponential function constants used for fitting. Because τ_{avg}depends on four fitted parameters; the uncertainty was obtained using standard error propagation:

$$\partial_{\tau\ avg} = \sqrt{\left(\frac{\partial\tau_{avg}}{\partial A_1}\partial A_1\right)^2 + \left(\frac{\partial\tau_{avg}}{\partial A_2}\partial A_2\right)^2 + \left(\frac{\partial\tau_{avg}}{\partial\tau_1}\partial\tau_1\right)^2}$$

Where, σ_{A1},σ_{A2} are fitting errors for weights of multiple exponential function constants and $\sigma_{\tau 1}$,$\sigma_{\tau 2}$ are fitting errors for lifetimes. These standard errors come directly from the nonlinear least-squares regression in OriginPro.

Table S1. Shows the surface atomic composition obtained from XPS survey spectra of $CsMnBr_3$, $CsFeBr_3$, and $CsNiBr_3$ nanocrystals. The presence of C, O, and N originates from oleic acid and oleylamine ligands used during colloidal synthesis.

Table S1. Surface elemental composition from XPS survey spectra of $CsMBr_3$ nanocrystals

Sample	Cs (%)	Br (%)	M (%)	C (%)	O (%)	N (%)
$CsMnBr_3$	3.95	12.91	1.72 (Mn)	76.08	2.33	3.01
$CsFeBr_3$	5.36	22.92	4.48 (Fe)	59.15	5.84	2.25
$CsNiBr_3$	4.73	20.32	3.60 (Ni)	63.39	3.56	4.40

Table S2-S4. High-resolution XPS fitting parameters for $CsMnBr_3$, $CsFeBr_3$, and $CsNiBr_3$ nanocrystals, including binding energy (BE), full width at half maximum (FWHM), and atomic percentage obtained from peak deconvolution. The results confirm the presence of Cs^+, Br^-, and the expected oxidation states of Mn^{2+}, Fe^{2+}, and Ni^{2+} within the perovskite lattice.

Table S2. High-resolution XPS fitting parameters of $CsMnBr_3$

Core level	Chemical state	Binding energy (eV)	FWHM (eV)	Atomic %
Br 3d	Bromide	68.8	2.1	12.91
C 1s	C-C	284.9	1.2	68.47
C 1s	C-O	286.2	1.2	7.61
N 1s	Organic N	399.6	1.7	0.51
N 1s	Ammonium	401.8	1.7	2.50
O 1s	C-O	532.0	1.6	1.54
O 1s	C=O	533.2	1.6	0.79
Mn $2p_{3/2}$	Mn^{2+} ($MnBr_2$)	641.7	2.8	1.72
Cs $3d_{5/2}$	CsBr	724.6	1.4	3.95

Table S3. High-resolution XPS fitting parameters of $CsFeBr_3$ nanocrystals

Core level	**Chemical state**	**Binding energy (eV)**	**FWHM (eV)**	**Atomic %**
Br 3d	Bromide	69.0	2.0	22.92
C 1s	C-C	284.9	1.1	55.31
C 1s	C-O	286.2	1.1	3.84
N 1s	Organic N	400.1	1.6	0.54
N 1s	Ammonium	402.1	1.6	1.71
O 1s	Metal oxide	530.5	1.3	1.47
O 1s	C-O	532.1	1.3	3.92
O 1s	C=O	533.5	1.3	0.45
Fe $2p_{3/2}$	Fe^{2+} ($FeBr_2$)	710.3	4.0	4.48
Cs $3d_{5/2}$	CsBr	724.6	1.3	5.36

Table S4. High-resolution XPS fitting parameters of $CsNiBr_3$ nanocrystals

Core level	**Chemical state**	**Binding energy (eV)**	**FWHM (eV)**	**Atomic %**
Br 3d	Bromide (Br^-)	68.9	2.3	20.32
C 1s	C-C	284.9	1.3	40.79
C 1s	C-O	286.1	1.3	15.64
C 1s	C=O	287.1	1.3	6.96
N 1s	Organic N	399.5	2.2	1.51
N 1s	Ammonium	402.0	2.2	2.89
O 1s	C-O	531.9	2.1	2.05
O 1s	C=O	533.5	2.1	1.51
Cs $3d_{5/2}$	CsBr	724.5	1.6	4.73
Ni $2p_{3/2}$	Ni^{2+} ($NiBr_2$)	855.8	2.2	3.60

Table S5: FTIR peak assignments to capping ligands

Wavenumber (cm^{-1})	Assignment to AO and OLA
2917	-CH_2- asymmetric stretch
2844	-CH_2- symmetric stretch
1707	C=O stretch
1458	-NH_2 bending

Table S6. FTIR peak assignments to capping ligands

Sample	Shifted band (cm^{-1})	Assignment	Interpretation
$CsMnBr_3$	1635 - 1645	Coordinated C=O / asymmetric COO^- stretch	OA bound to Mn surface
$CsNiBr_3$	1625 - 1635	Coordinated C=O / COO^- stretch	Stronger interaction with Ni
$CsFeBr_3$	1640 -1650	Coordinated C=O / COO^- stretch	OA coordinated to Fe

Key interpretation:

1707 cm^{-1} (free OA) to 1625 -1650 cm^{-1} ($CsMBr_3$ NCs), the red shift of 60 - 80 cm^{-1} indicates coordination of oleate to the metal ions on the nanocrystal surface. This shift occurs because electron density is delocalized over the carboxylate group. As the C=O bond order decreases, the vibration frequency decreases. Additional peaks in $CsMnBr_3$, $CsNiBr_3$, $CsFeBr_3$ (1500 -1000 cm^{-1} region)

These peaks are typically due to:

a) C=C stretching (~1600 - 1500 cm^{-1})

From the unsaturated bond in oleic acid /oleylamine.

b) C-N stretching (~1200 -1350 cm^{-1})

Associated with amine groups from oleylamine.

c) C-O stretching (~1000 - 1200 cm^{-1})

From the carboxylate group of oleic acid interacting with the metal surface. **Low-frequency region (< 600 cm^{-1})**

Often weak or outside the plotted range.

Assignment:

- **M-Br lattice vibrations** (Mn-Br, Ni-Br, Fe-Br).

These vibrations confirm the formation of the metal bromide perovskite lattice.